WPMAT-CPR(17) 17003

A Litnovsky et al.

New Oxidation Resistant Tungsten Alloys for use in the Nuclear Fusion Reactors

Preprint of Paper to be submitted for publication in Proceeding of 16th International Conference on Plasma-Facing Materials and Components for Fusion Applications

This work has been carried out within the framework of the EUROfusion Consortium and has received funding from the Euratom research and training programme 2014-2018 under grant agreement No 633053. The views and opinions expressed herein do not necessarily reflect those of the European Commission.

New Oxidation Resistant Tungsten Alloys for Use in the Nuclear Fusion Reactors

A. Litnovsky[a,1], T. Wegener[a], F. Klein[a], Ch. Linsmeier[a], M. Rasinski[a], A. Kreter[a], X. Tan[a,b], J. Schmitz[a], J.W. Coenen[a], Y. Mao[c], J. Gonzalez-Julian[a] and M. Bram[a]

[a]*Forschungszentrum Jülich GmbH, Institut für Energie- und Klimaforschung, 52425 Jülich, Germany;*

[b]*School of Materials Science and Engineering, Hefei University of Technology, Hefei 230009, China;*

[c]*Institute for Materials Applications in Mechanical Engineering, RWTH Aachen University, 52062 Aachen, Germany*

Abstract

Smart tungsten-based alloys are under development as plasma-facing components for a future fusion power plant. Smart alloys are planned to adjust their properties depending on environmental conditions: acting as a sputter-resistant plasma-facing material during plasma operation and suppressing the sublimation of radioactive tungsten oxide in case of an accident on the power plant. New smart alloys containing yttrium are presently in the focus of research. Thin film smart alloys are featuring an remarkable 10^5-fold suppression of mass increase due to an oxidation as compared to that of pure tungsten at 1000°C. Newly developed bulk smart tungsten alloys feature even better oxidation resistance compared to that of thin films. First plasma test of smart alloys under DEMO-relevant conditions revealed the same mass removal as for pure tungsten due to sputtering by plasma ions. Exposed smart alloy samples demonstrate the superior oxidation performance as compared to tungsten-chromium-titanium systems developed earlier.

I. Introduction and motivation

Plasma-facing components (PFCs) in the future fusion power plant will be exposed to extremely high plasma particle fluence, intensive neutron irradiation and heat loads exceeding those in any existing fusion experiment by orders of magnitude. Conventional materials will unlikely be able to accommodate the envisaged loads and fluxes simultaneously [1, 2]. New advanced plasma-facing materials have to be developed for the fusion power plant application.

[1] Corresponding author:
Dr. Andrey Litnovsky
Forschungszentrum Jülich GmbH, Institut für Energie- und Klimaforschung – Plasmaphysik,
Partner of the Trilateral Euregio Cluster (TEC),
52425 Jülich, Germany.
Tel.: +49 (0)2461 61 5142
E-mail address: a.litnovsky@fz-juelich.de

One example of the current physics and technology challenges is the choice of the armor material for the first wall of the future fusion power plant, like DEMOnstration fusion power plant (DEMO). Due to a number of the advantageous features such as a high melting point, low sputtering coefficient by plasma ions, low retention of the radioactive fusion fuel –tritium, as well as due to its excellent thermal conductivity, tungsten (W) is currently deemed as the best material solution for the first wall of existing and future fusion experiments, like ITER.

However, in the power plant the application of pure W will be challenging. In case of a severe catastrophic scenario, comprising the so-called Loss-of-Coolant Accident (LOCA) with simultaneous air ingress, an active cooling of the first wall will likely be destroyed. The tungsten first wall armor would heat up due to nuclear decay heat reaching the peak temperature of up to 1200^{o}C depending on current DEMO design [3]. According to the estimates [3] such a temperature could last for several months. At such conditions, the neutron-irradiated, radioactive tungsten forms a volatile tungsten oxide, which may become released into environment. The recent estimates predict the tungsten oxide sublimation rate of up to 100 kg per hour – a rate which cannot be tolerated.

The so-called self-passivating "smart" advanced tungsten-based alloys are under development to address this issue. Self-passivating systems introduced for tungsten by F. Koch and H. Bolt [4] are aimed to accommodate their properties to the current environmental conditions. During the regular plasma operation, plasma ions and neutrals of high energy may sputter the surface of the smart alloy. The preferential sputtering will first remove the lighter candidate alloying elements: titanium (Ti), chromium (Cr) and yttrium (Y) from the plasma-exposed surface thus providing almost pure tungsten surface facing the plasma. In case of an accident, the alloying elements remaining in the bulk of the smart alloy system will form their own dense oxides, protecting tungsten from sublimation.

Previous research was performed with several binary and ternary alloy system using silicon (Si), chromium and titanium as alloying elements [4-6]. The W-Cr-Ti system was shown to have the longest and the most effective suppression of tungsten oxidation among all studied alloy systems.

At the same time, an addition of yttrium (Y) was proven to have an extremely positive effect on the stability and oxidation resistance of the stainless steels. Based on available experience with steel optimization and taking into account the proven advantages of Y [7-14], summarized in [15] it was decided to focus efforts on studies of Y-containing smart alloys.

II. Thin film smart alloys

Initial studies were performed on thin film smart alloy systems. Thin films were produced using the multi-magnetron facility PREVAC at the Forschungszentrum Jülich. Ideally homogenous smart alloy coating was obtained by simultaneous deposition of three materials: W, Cr and Y were deposited onto sapphire substrates of the 12 mm diameter, placed onto a rotating sample table below the targets. By

individual varying the operating regime of each target, it became possible to produce the thin film alloy system with the pre-programmed elemental composition and with desired thickness of up to 7 µm. The standard thickness of the thin film smart alloy systems was about 3 µm.

Several experimental techniques were applied for studies of smart alloys. The oxidation tests were performed using the symmetrical double oven TGA system Setaram TAG 16. Oxidation exposures in humid atmosphere were realized by joining the steam generator Wetsys from Setaram to the TGA system. The integral mass change was monitored with the Sartorius MSA225P microbalance with a resolution of 10 µg. Film thickness was measured with mechanical stylus Dektak 6M and independently using Focused Ion Beam (FIB) system. Surface morphology was monitored using the scanning electron microscope (SEM). The combined SEM-FIB system Carl Zeiss CrossBeam XB540 equipped with Energy Dispersive X-ray analysis system (EDX) and with Electron BackScattering Diffraction (EBSD) systems was used for investigations. When needed, an inverse optical microscope Carl Zeiss Axio Observer z11n was used to investigate morphology changes. All studies reported in this paper were made at the prescribed fixed temperature.

During the oxidation, the mass change of the sample was recorded. In case of passivation an oxidation process is driven by the diffusion of oxygen and alloying elements through the protective layer. If the protective layer is stable and there is no cracking and/or delamination, the mass change Δm is proportional to the increase of the volume of oxide. Since oxidation is controlled by diffusion, the increase of the volume is proportional to the diffusion depth of oxidation:

$$l=(Dt)^{1/2} \qquad (1)$$

where D is the diffusion coefficient and t is the oxidation time [10]. From the formula (1) we can infer, that the change of the volume and the corresponding mass change is proportional to the square root of time demonstrating the so-called “parabolic behavior”.

The studies of the smart alloys were started with the optimization of elemental composition of the thin film systems. Thin smart alloys with different concentrations of alloying elements were produced. Then these systems underwent the oxidation under identical conditions. This controlled isothermal oxidation was made at the temperature T=1000^{o}C in the gas mixture containing 20 vol.% of oxygen (O_2) and 80 vol.% of argon (Ar) at pressure of 1 bar.

The results of elemental composition scan are published in [16]. The smart alloy with the composition W-11.6Cr-0.6 Y demonstrated the lowest oxidation rate. Here and further in the paper the values in front of the element symbol represent the fraction of an element in the alloy in wt.%. i.e. an alloy W-11.6Cr-0.6 Y consists from 11.6 wt.% of Cr and 0.6 wt.% of Y with tungsten constituting the rest.

The optimized W-Cr-Y thin film alloy was than compared with the best binary (W-Cr) and ternary (W-Cr-Ti) systems studied so far. The results of the oxidation of these three systems and thin film pure W sample are provided in Fig. 1 as dependence of the mass gain on the time of exposure. As it can be

inferred from the Fig. 1, the W-Cr-Y system demonstrated the lowest oxidation rate with the parabolic dependency on time, whereas both the W-Cr-Ti system exhibit the signs of the breakaway oxidation after approximately 600 seconds of oxidation and binary W-Cr system – after ~ 300 seconds already.

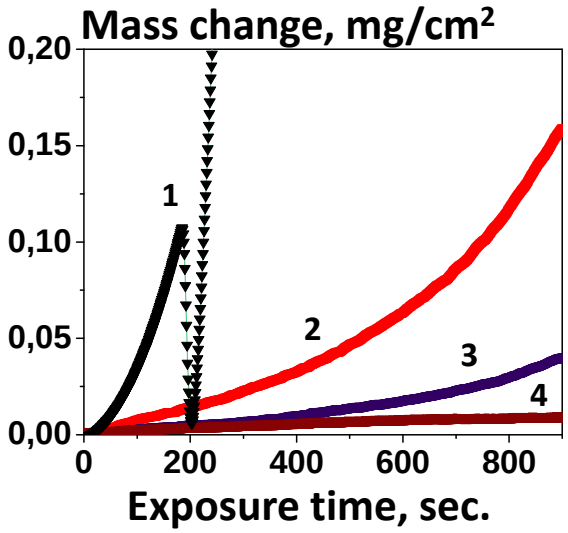

Figure 1. *Dependence of the mass gain on oxidation time for pure W and thin film smart alloys: 1) pure W, 2) W-10.3Cr, 3) W-10.7Cr-1.1Ti, 4) W-11.6Cr-0.6Y*

The reason for such a drastic difference can be inferred from the analyses of the structure of the formed protective layer and the material of the smart alloy beneath affected by the oxidation. The respective results of the FIB investigations are presented in Fig. 2.

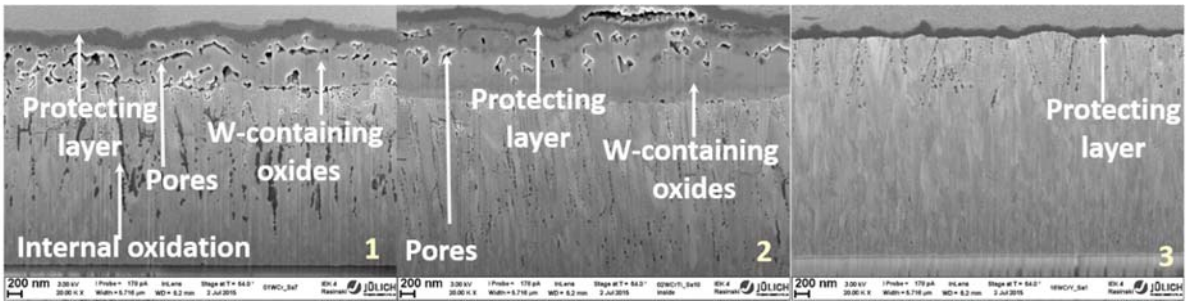

Figure 2. *Cross-section of the thin film smart alloys after 15-minute oxidation in 80 vol.% Ar + 20 vol.% at 1000°C: 1) W-10.3Cr, 2) W-10.7Cr-1.1Ti, 3) W-11.6Cr-0.6Y*

In case of the binary system W-10.3Cr, Fig 2.1., the clearly pronounced in-depth oxidation was noticed together with mixed W-containing W-Cr oxides covered by the protecting Cr_2O_3 layer. The structure of the protective layer however, contained a large number of pores, which obviously negatively influenced the oxidation behavior presented on Fig. 1, curve 1. The situation is significantly improved with the introduction of a second alloying element. The structure of oxidized ternary system W-10.7Cr-1.1Ti is presented in Fig.2.2. The in-depth oxidation noticed for binary system, was almost fully suppressed, the amount of pores decreased, but the pores did not disappear completely. The mixed

oxides at the interface between the protective layers and the smart alloys are still visible. This all led to the improved oxidation resistance, Fig.1 curve 2, yet resulting to the aforementioned disruption into breakaway oxidation regime. Finally, for a new W-11.6Cr-0.6Y system, the difference in morphology of exposed surface was rather striking. Neither mixed oxides, nor pores and negligible in-depth oxidation was detected. The protective Cr_2O_3 layer was much thinner and obviously, denser than that for all aforementioned samples.

As a next step, studies of oxidation-resistance of the thin film systems were performed in humid atmosphere to approach conditions expected in DEMO during an accident. For these tests, the steam generator WetSys was providing the mixture: 80 vol.% of N_2 + 20 vol. % of O_2 with the relative humidity of 70% at 1 bar. The humid synthetic air was fed to the interaction volume where the sample was located. The oxidation took place at 1000°C. The dedicated studies show no effect of nitrogen on the oxidation performance at the experimental conditions.

The results of the oxidation of the W-11.6Cr-0.6Y smart alloy thin film system and the pure tungsten sample under aforementioned conditions are provided in Fig. 3.

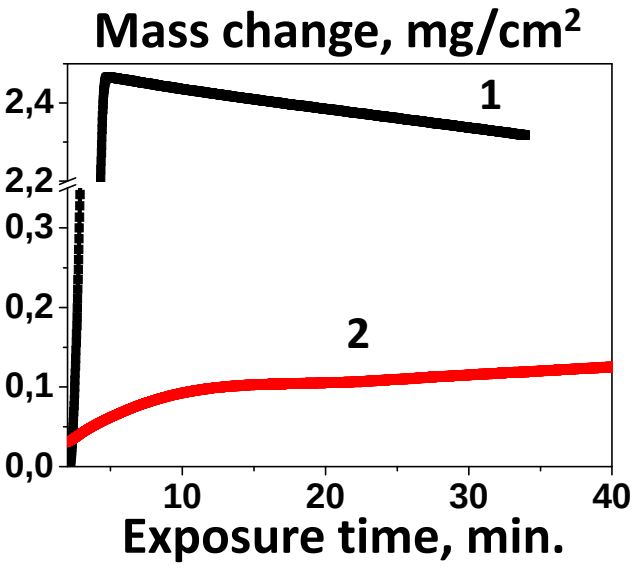

Figure 3. *Evolution of mass change with time during oxidation in 80 vol.% N_2 + 20 vol.% O_2 at 1000°C fed at 1 bar with 70% relative humidity a 40°C to: 1) pure W, 2) W-11.6Cr-0.6Y smart alloy. Oxidation exposure carried out at 1000°C. Studies were performed on thin film samples.*

The remarkably quick complete oxidation is followed by a slow mass decrease due to the sublimation of the fully oxidized sample. On the contrary, the smart alloy system show the parabolic oxidation coupled with a slight "bump" at approximately 20 minutes of exposure. The most probable reason of such a bump is local oxidation and eventually, sublimation of the affected material. The presence of W-containing oxides on top of the protective layer, detected during the FIB investigations, supports the sublimation as the most probable reason for the observed mass decrease. Nevertheless, despite

of local limited mobilization of the smart alloy, the oxidation resistance in humid atmosphere was drastically improved in comparison to that of pure W [17]. With the promising results achieved on model thin film systems, it was decided to start production of the DEMO-relevant bulk smart alloy samples.

III. Bulk smart alloys

The production of bulk smart alloys consists from two main stages:

1) Mechanical alloying of the elementary powders

2) Sintering of the alloyed powder

In the first stage, the elementary powders are milled together under argon atmosphere using a planetary mill system. The aim of this stage is to create a solid solution of tungsten and alloying element(s). In our studies, the planetary mill system Retsch PM400 was used to create the mechanically alloyed powder. The elementary W, Cr and Y powders were poured into 250 ml tungsten carbide milling jar. The jar was filled with hard tungsten carbide balls with a diameter of 10 mm. The ball-to-powder ratio was 5:1. The milling was undertaken at room temperature with 250 rpm speed for up to 60 hours. During the exploration of the mechanical alloying of tungsten-containing powder, fractions of powder were taken out from the jar to determine the degree of the alloying using X-Ray Diffraction (XRD) system D8 Advance by Bruker. In addition, FIB sectioning of the powder particles was performed to investigate the homogeneity of the material after milling. An XRD spectra of elementary powders at different times of milling are presented in Fig. 4. According to the XRD results, a complete mechanical alloying was attained after 60 hours of continuous milling as can be inferred from the completely disappeared peaks of the elemental W and Cr in the resulting powder.

At the same time the sectioning of the powder particles, provided an evidence of the creation of a completely homogenous distribution of alloying elements in the powder particle. Due to ability of producing the homogenous solid solution of tungsten and alloying elements at room temperature, the first stage of manufacturing is considered as necessary and is present in all techniques for producing bulk smart alloys.

However, there are different ways of realizing the second stage of production of the smart alloy systems. In [18-21], bulk smart alloy samples were produced using a hot isostatic pressing (HIP). The recent results obtained on bulk W-Cr-Y systems however, demonstrate the massive transport of tungsten through the protective oxide layer [21]. The existing inhomogeneity of the elemental distribution along such samples may be responsible for the noticed degradation of oxidation resistance in comparison to that of the thin film samples. The aforementioned studies suggest the crucial role of the highest homogeneity of the elements along the alloy coupled with the smallest grain size of the alloy.

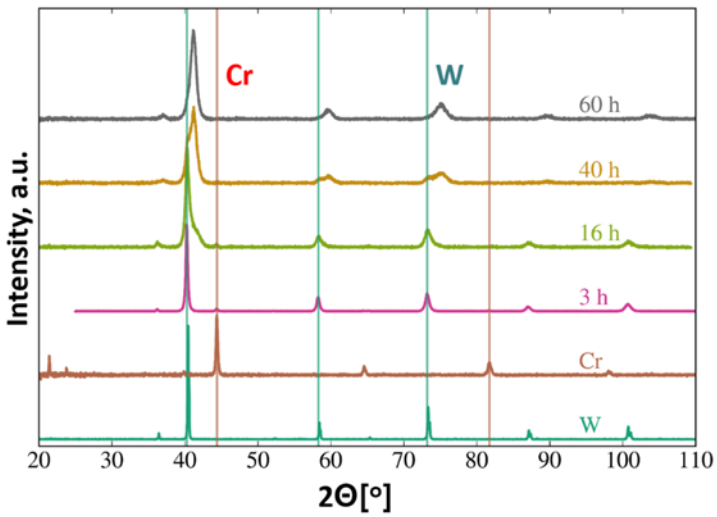

Figure 4. *XRD spectra of tungsten and chromium, and evolution of mechanical alloying with milling time.*

In order to attain such conditions, we have decided to apply an alternative technique for the production of bulk smart alloy systems: Spark Plasma Sintering (SPS) also known as Field-Assisted Sintering Technology (FAST) [22]. In FAST, the powder is placed in a graphite die between two graphite punches, which apply uniaxial pressure during the thermal treatment. The maximal pressure is typically < 100 MPa, meanwhile the maximum temperature of the FAST process is around 2200 °C. There is a Joule heating caused by the pulsed DC current with low voltage and high intensity (10^3 A) through the graphite system. The main advantages of FAST are:

i) High heating rates: heating rates faster than 100 K/min are typically achieved in FAST due to the pulsed DC current. This is highly beneficial for the reduction of the time at high temperatures, leading to recrystallization of the sample and degrading the required homogeneity.

ii) Pressure: uniaxial pressure during the thermal cycle promotes the densification, reducing the maximal temperature required to fully densify the material.

iii) Reduction of time: the fast heating rates and short isothermal holding time (~ min) to densify a material reduce the time that the sample is at high temperature. This effect saves a lot of energy and leads to tailor the final microstructure, such as reduction/inhibition of the grain growth.

iv) Ability of operating below the recrystallization temperature: The reduction of the maximal temperature due to the uniaxial pressure and the DC current lead to densify materials at lower temperatures than by other sintering techniques. As a result, it is possible to densify materials below the recrystallization temperature and/or degradation of some compounds.

A FAST/SPS facility FCT-HDP5 from FCT-Systeme was used in our experiments. In order to tune up the FAST technique for production of bulk smart alloys the six-stage optimization procedure was developed and realized. During the procedure, the most essential parameters of the FAST technique, such as:

1. Temperature ramp, K/min
2. Maximum temperature

   and
3. Holding time at the maximum temperature

were scanned. The applied pressure of 50 MPa was kept constant in all studies. The W-11.4Cr-0.6Y mechanically alloyed powder was used in all FAST studies. The summary of applied regimes is provided in table 1.

Table 1. *Parameters of optimization of FAST process*

Sample	Heating ramp, ^{o}C/min	Holding time, min	Maximum temperature, ^{o}C.
FAST 1	200	1	1550
FAST 2	100	1	1550
FAST 3	100	1	1460
FAST 4	200	1	1460
FAST 5	200	0.5	1460
FAST 6	200	0	1460

After every optimization step, the produced bulk smart alloy ingot was taken from the die, cut into small pieces with a diamond saw, ground with a diamond paper until the surface roughness of ~ 30 nm and ultrasonically cleaned. Then the resulting bulk samples were investigated using SEM and FIB in order to evaluate the elemental composition, homogeneity and the grain size. The overview of FIB investigations is presented in Fig.5. for samples FAST 1 – FAST 6.

As it can be clearly seen from the Fig. 5, avoiding the holding time and imposing the steepest temperature ramp enabled us achieving a very fine structure with compact nanograins with the size of < 100 nm and the finest Y distribution along the boundaries of formed nanograins. At the final step, produced bulk samples of each time were exposed under identical conditions in the dry oxidative environment.

In all samples, fine yttria particles with a size of < 150 nm were concentrated at the grain boundaries of the W-Cr solid solution in a complete similarity as described in [15]. The results of oxidation studies are presented in Fig. 6. Generally, the oxidation characteristics of the newly produced bulk smart alloys were even better that those from the reference thin films.

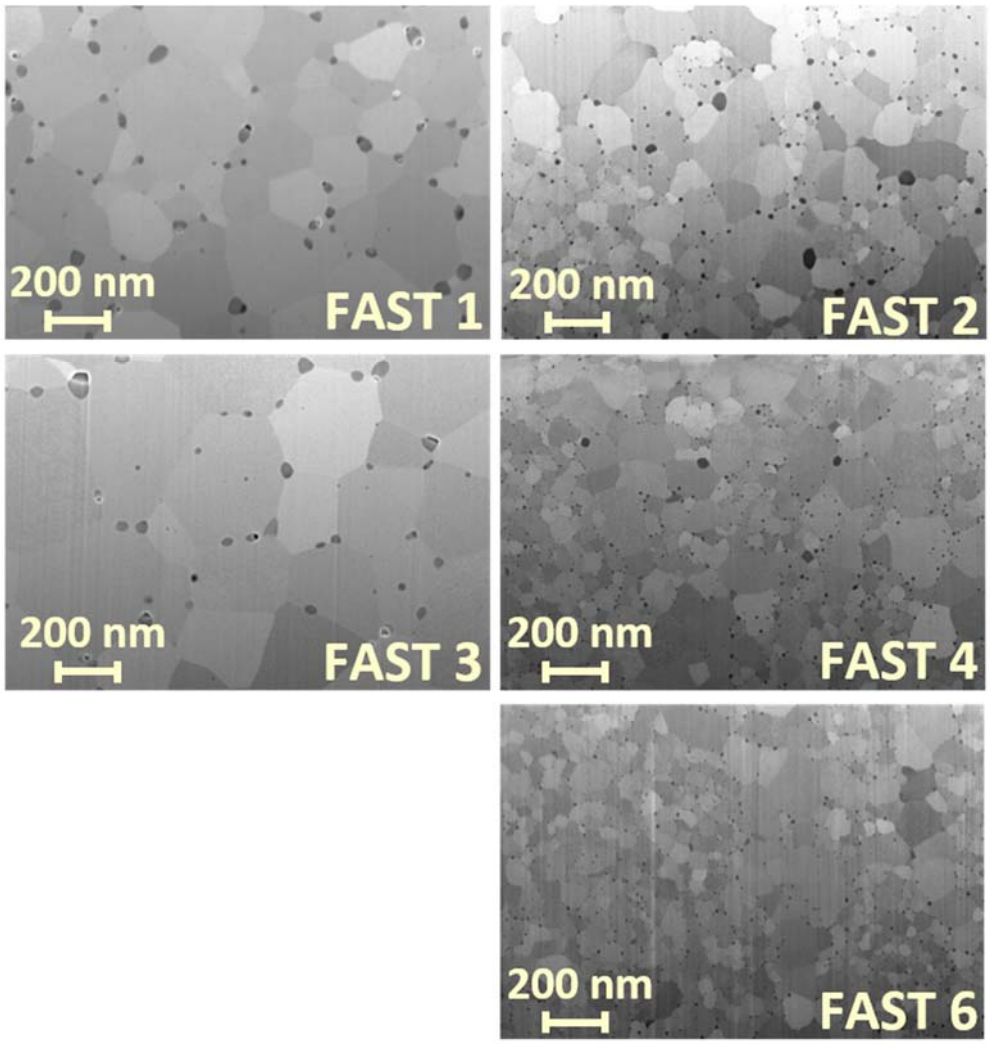

Figure 5. *Grain structure of the samples produced using different FAST scenarios.*

From Fig.6 it can be inferred that the sample FAST 6, made with temperature ramp of 200 K/min without any holding time and with the maximum temperature of 1460^{o}C demonstrate the unprecedentedly low oxidation rate.

IV. First complete performance test: plasma exposure and accidental conditions

Since smart alloys are planned to be employed both during the regular plasma operation and in accidental conditions, the combined testing of smart alloys under plasma impact followed by the oxidation of the exposed samples is crucially important. The first such a combined test with two FAST1 samples: SA1 and SA2 was performed recently.

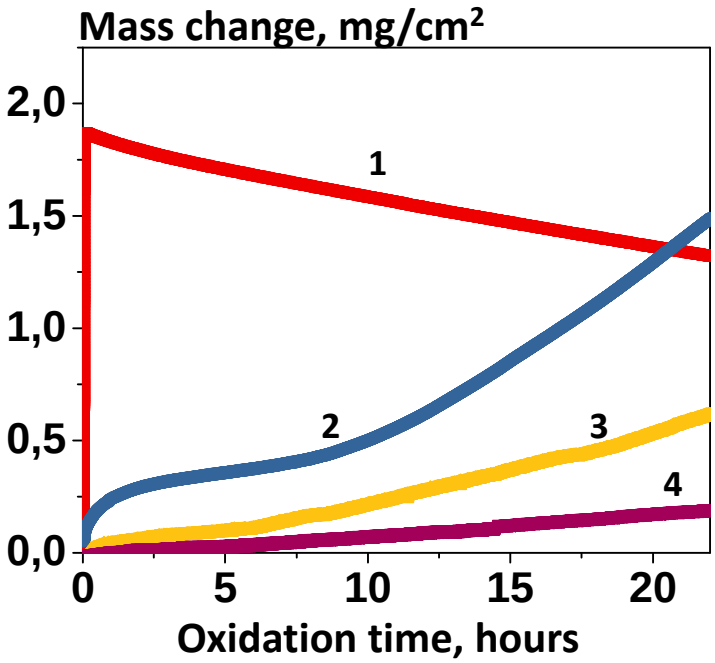

Figure 6. *Mass change during the oxidation process: 1) for the pure thin film W sample, 2) for the reference thin film W-11.6Cr-0.6Y smart alloy, 3) for FAST 1 sample and 4) for FAST 6 sample. Oxidation took place in the atmosphere consisting from 80 vol.% of Ar + 20 vol. % of O_2 at 1 bar and 1000^{o}C.*

The plasma exposure was conducted in identical manner as the recent study of the W-Cr-Ti system described in [23]. Two FAST samples of W-11.4Cr-0.4Y smart alloys were manufactured from the FAST ingots using spark erosion. Two samples from pure W manufactured according to ITER specification [24] were used for a direct comparison. Plasma facing sides of all the samples under study were ground with a diamond paper to the roughness of 20-30 nm. Series of pre-characterizations were made on all studied samples including:

1. Weight measurements for evaluation of sputtered materials
2. SIMS measurements for understanding the initial elemental composition
3. Stylus profiler measurements of surface roughness Ra were made on several locations
4. SEM scans were made for investigation of initial morphology of the surface
5. FIB measurements were made to study the grain size, homogeneity study and for making markers needed for the direct evaluation of sputtered material

The photo of the smart alloy sample along the scheme of the measurement locations is provided in Fig. 7.

Smart alloy and pure tungsten reference samples were installed in the sample holder and exposed to steady-state deuterium plasma in the PSI 2 linear plasma device [25]. Plasma parameters were evaluated using the moveable Langmuir probe. Electron temperature was T_e~6-8 eV depending on radial position. Active biasing was applied to the sample holder. The energy of impinging ions was ~

220 eV. The samples were actively heated to the temperature of 620°C-650°C. The temperature was monitored with the thermocouple installed on the backside of one of the samples. Ion energy and the temperature during exposure provided a conservative estimate of the environment expected in DEMO [26]. The total exposure duration was four hours 36 minutes. The accumulated fluence was $1x10^{22}$ ion/cm^2.

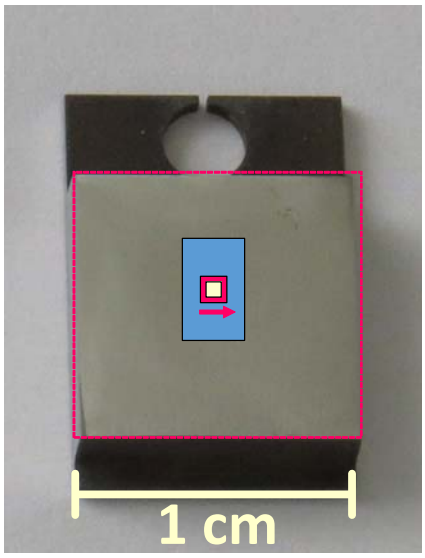

Figure 7. *Smart alloy sample produced for plasma exposure: a view of a sample with the measurement locations: arrow show the location of surface roughness scan with stylus profiler, large area is the location of SEM surveys, smaller square in the middle is the location of SIMS depth profiles and the smallest square shows the location of FIB cut.*

After exposure, the surface characterization described above was repeated on all exposed samples. A brief summary of obtained results is provided in table 2. From the obtained data, it can be confirmed that the mass loss of both pure W samples and smart alloys was nearly identical. The removed material after exposure accounted for ~ 450 nm for pure W samples and for ~ 870 nm for smart alloys. The surface roughness increased from ~ 20 to ~ 50 nm on the majority of studied locations. Generally, newly developed bulk W-Cr-Y systems even at this early stage of development, already demonstrated very good plasma performance. Further investigations on exposed samples are under way.

Table 2. *Main parameters of exposed pure tungsten and smart alloy samples*

Sample	Mass loss [μg]	$R_{a,\ before}$ [nm]	$R_{a\ ,\ after}$ [nm]	Eroded material, nm
W1	1200±10	30±7	141 ±55	460
W2	1093±10	24±8	52± 49	440
SA1	1287±10	22±5	46±25	860
SA2	1223±10	24±9	47±32	870

In order to evaluate impact of plasma on the oxidation resistance, one of plasma-exposed smart alloy samples underwent the isothermal oxidation at 1000^{o}C, in the gas mixture, containing 20 vol. % of O2 and 80 vol.% of Ar at 1 bar. The results of this oxidation and their comparison with data from non-exposed FAST sample is presented in Fig. 8. In addition, the oxidation curve for pure W along with the oxidation curves of the previous W-Cr-Ti systems reported earlier in [22] are provided in Fig 8.

The analysis of obtained dependencies does show the decrease of oxidation resistance after plasma exposure calling for the future necessary further optimization of smart alloy systems. At the same time the results obtained with W-Cr-Y systems are by far superior than those obtained with W-Cr-TI alloys studied recently representing a very promising result.

Summary

New advanced tungsten-based smart alloys are needed to ensure the intrinsic safety for a future fusion power plant, like DEMO. Smart alloys have to combine acceptable plasma performance with suppressed oxidation in case of an accident. The research program on smart alloys at Forschungszentrum Jülich has started with detailed investigation of W-Cr-Y alloy systems. The first studies made on thin film smart alloys demonstrate a remarkable 10^5-fold suppression and much better durability of smart alloy systems as compared to that of a pure tungsten.

The first bulk smart alloy samples of DEMO-relevant size became available as a result of the powder-metallurgical route of manufacturing. At a first stage, the applied mechanical alloying was applied to the elementary powders of tungsten and the alloying elements. As a result of 60-hour milling, a solid solution of W-Cr was attained at room temperature. The mechanically alloyed powder was then sintered using an advanced field-assisted sintering technique (FAST). Bulk samples with 99.8% of nominal density, featuring a fine nano-grain structure with the grains of 100-200 nm and homogenous distribution of yttria along the W-Cr grain boundaries, were obtained. The measured oxidation resistance was clearly superior even in comparison to the reference thin film systems.

First combined tests of newly developed smart alloys were performed. These tests comprised exposure of smart alloys in steady-state deuterium plasma followed by the controlled oxidation of the exposed samples. The exposure was made in the linear plasma device PSI 2. Smart alloy samples were exposed together with pure W samples under identical plasma conditions. The exposure temperature (~630^{o}C) and the energy of impinging ions (220 eV) provided conditions for a rather conservative estimate of performance of smart alloys under DEMO-relevant conditions. In the course of exposure, smart alloys exhibit the same mass removal by the plasma, as a pure tungsten samples. Volumetric loss of smart alloy (850 nm) was about twice as much as that of pure tungsten (460 nm), as expected. Similar

evolution of the surface roughness of smart alloy and pure tungsten in the course of exposure was detected.

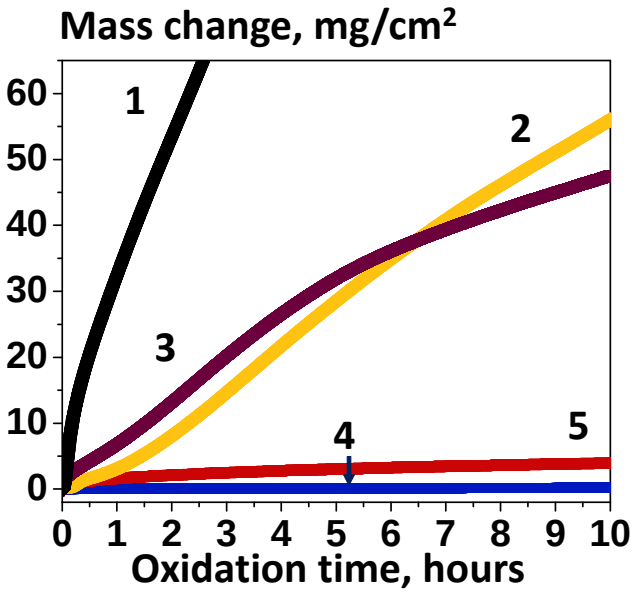

Figure 8. *Mass change during the oxidation process: 1) for the pure W sample, 2) for the reference W-10Cr-2Ti smart alloy [22], 3) the W-10Cr-2Ti smart alloy exposed in plasma [22], 4) for the reference W-11.6Cr-0.6Y smart alloy and 5) for the W-11.6Cr-0.6Y smart alloy exposed in plasma. Oxidation took place in the atmosphere consisting from 80 vol.% of Ar + 20 vol. % of O2 at 1 bar and 1000°C.*

The subsequent oxidation of exposed smart alloy sample revealed a superior oxidation resistance as compared with former ternary W-Cr-Ti system. At the same time, the oxidation resistance of the W-Cr-Y slightly degraded as compared to non-exposed sample calling for further optimization of produced smart alloy systems.

Outlook

Future studies will be focused on increasing of the oxidation resistivity of the bulk smart alloy system. Plasma exposures with gas seeding will be performed for a further investigation of impact caused by plasma on sputtering of smart alloys and their oxidation performance. New oxidation exposures will be made in humid air atmosphere in order to approach the accidental condition in DEMO. Effort will be put on studies and if necessary, improvement of thermo-mechanical properties of the smart alloy systems. Furthermore, it is planned to study the effect of neutron irradiation on mechanical properties of smart alloys in future.

Acknowledgments

A part of these studies has been carried out within the framework of the EUROfusion Consortium and has received funding from the Euratom research and training programme 2014-2018 under grant agreement No. 633053. The views and opinions expressed herein do not necessarily reflect those of the European Commission.

References:

[1] M. Rieth, S.L. Dudarev, S.M. Gonzalez de Vicente et al, J. Nucl Mater. 432 (2013) 482;

[2] J. W. Coenen, S. Antusch, M. Aumann et al., Phys. Scr. T167 (2016) 014002;

[3] D. Maisonner et al, A Conceptual Study of Commercial Fusion Power Plants, Final Report, 2005, EFDA-RP-RE-5.0;

[4] F. Koch and H. Bolt Phys. Scr. T128 (2007)100;

[5] F. Koch, S. Köppl and H. Bolt, J. Nucl. Mater. 386–388 (2009) 572-574;

[6] F. Koch, J. Brinkmann, S. Lindig, T.P. Mishra and Ch. Linsmeier, Phys. Scr. T145 (2011) 014019;

[7] K. Przybylski, A. J. Garratt-Reed, and G. J. Yurek. Grain boundary segregation of yttrium in chromia scales. Journal of The Electrochemical Society, 135(2): 509517, 1988;

[8] M.F. Stroosnijder, et al. The inuence of yttrium ion implantation on the oxidation behaviour of powder metallurgically produced chromium. Surf. and Coat. Technology, 83, 205;

[9] N. Birks, G.H. Meier, and F.S. Pettit “Introduction to the High-Temperature Oxidation of Metals”, Cambridge University Press, 2006;

[10] R. Mevrel et al., Cyclic oxidation of high-temperature alloys Mater. Sci. Technol. 1987;

[11] R. Bürgel, H. J. Maier, and T. Niendorf. Handbuch Hochtemperatur-Werkstofftechnik. PRAXIS, 2011;

[12] “The role of active elements in the oxidation behavior of high temperature metals and alloys” ed. E. Lang, 1989, p. 39;

[13] N. B. Pilling and R. E. Bedworth J. Inst. Met 29 (1923), S. 529-591;

[14] I. Barin in collaboration with Gregor Platzk “Thermomechanical data of pure substances”, Third edition, Weinheim ; New York ; Base ;Cambridge ; Tokyo : VCH, ISBN 3-527-28745-0;

[15] A. Litnovsky, T. Wegener, F. Klein et al., Plasma Phys. and Contr. Fusion 59 (2017) 064003, doi: https://doi.org/10.1088/1361-6587/aa6948

[16] T. Wegener, A. Litnovsky, F. Klein et al., Nucl. Materials and Energy, 9 (2016) 394–398, http://dx.doi.org/10.1016/j.nme.2016.07.011

[17] T. Wegener, F. Klein, A. Litnovsky et al., "Development and analyses of self-passivating tungsten alloys for DEMO accidental conditions", presented at the Symposium on Fusion Technology (SOFT 2016), Prague, Czech Republic, September 5-9, 2016, O2B.2.

[18] S. Telu, R. Mitra and S.K. Pabi, Metallurgical and Materials Transactions A (2015) doi: 10.1007/s11661-015-3166-z;

[19] P. Lopez-Ruiz, N. Ordas, N, S. Lindig et al Phys. Scr. T145 (2011) 014018

[20] A. Calvo, C. García-Rosales, F. Koch et al., Nucl. Mater. and Energy 9 (2016) 422, http://dx.doi.org/10.1016/j.nme.2016.06.002

[21] A. Calvo, C. Garcia-Rosales, N. Ordas et al., "Self-passivating W-Cr-Y alloys: characterization and testing", presented at the Symposium on Fusion Technology (SOFT 2016), Prague, Czech Republic, September 5-9, 2016, P2-177, accepted for publication in Fus. Eng. and Design;

[22] O. Guillon, J. Gonzalez-Julian, J., Dargat et al., Advanced Engineering Materials, issue 16, vol. 7 (2014) 830

[23] A. Litnovsky, T. Wegener, F. Klein et al, "Smart alloys for a future fusion power plant: First studies under stationary plasma load and in accidental conditions" available online in Nuclear Materials and Energy, http://dx.doi.org/10.1016/j.nme.2016.11.015;

[24] ITER document: "Material Specification for the Supply of Tungsten Plates for the ITER Divertor", IDM No.: ITER_D_2EDZJ4

[25] A. Kreter, C. Brandt, A. Huber et al., Fusion Sci. Technol. 68(2015)8

[26] Yu. Igitkhanov, B. Bazylev, I. Landman and R. Fetzer, KIT Scientific report 7637, p. 20